Supplementary Material for

λ/20-thick cavity for mimicking electromagnetically induced transparency at telecommunication wavelengths

Hua Lu,[*] Shouhao Shi, Dikun Li, Shuwen Bo, Jianxu Zhao, Dong Mao, and Jianlin Zhao[*]

MOE Key Laboratory of Material Physics and Chemistry under Extraordinary Conditions, Key Laboratory of Light-Field Manipulation and Information Acquisition, Ministry of Industry and Information Technology, and Shaanxi Key Laboratory of Optical Information Technology, School of Physical Science and Technology, Northwestern Polytechnical University, Xi'an, 710129, China

*[*]Email: hualu@nwpu.edu.cn; jlzhao@nwpu.edu.cn*

Supplementary Figures
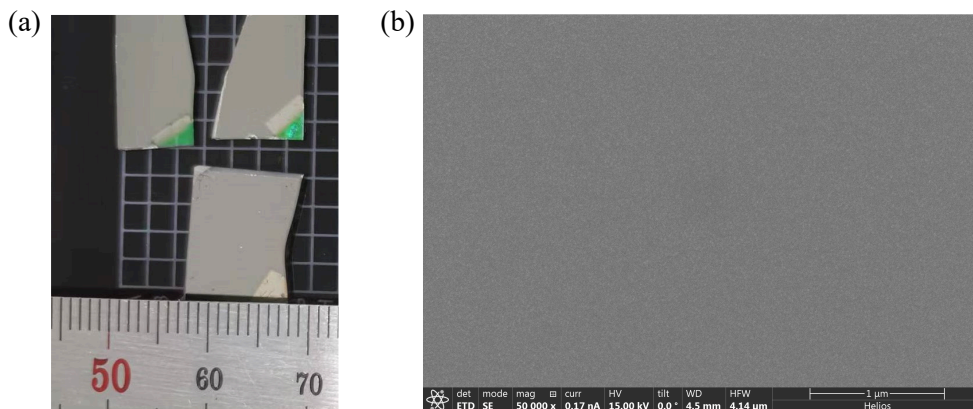
Fig. S1 (a) Optical images of Bi_2Te_3 TI nanofilms grown on the silver/1D photonic crystal and silver/SiO_2 structures. (b) SEM image of a MS-grown Bi_2Te_3 nanofilm.
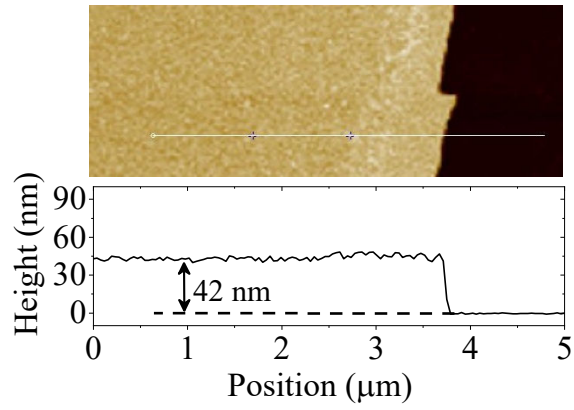
Fig. S2 AFM image of a 42 nm Bi_2Te_3 TI film and the height profile along the white line.
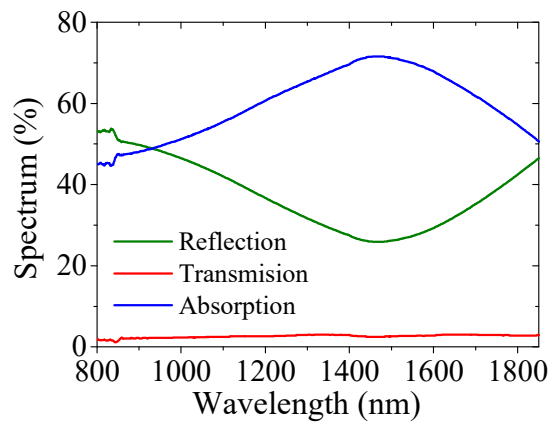

Fig. S3 Experimentally measured reflection, transmission, and absorption spectra of the Bi_2Te_3 TI nanocavity with a 42 nm Bi_2Te_3 film when t=30 nm.
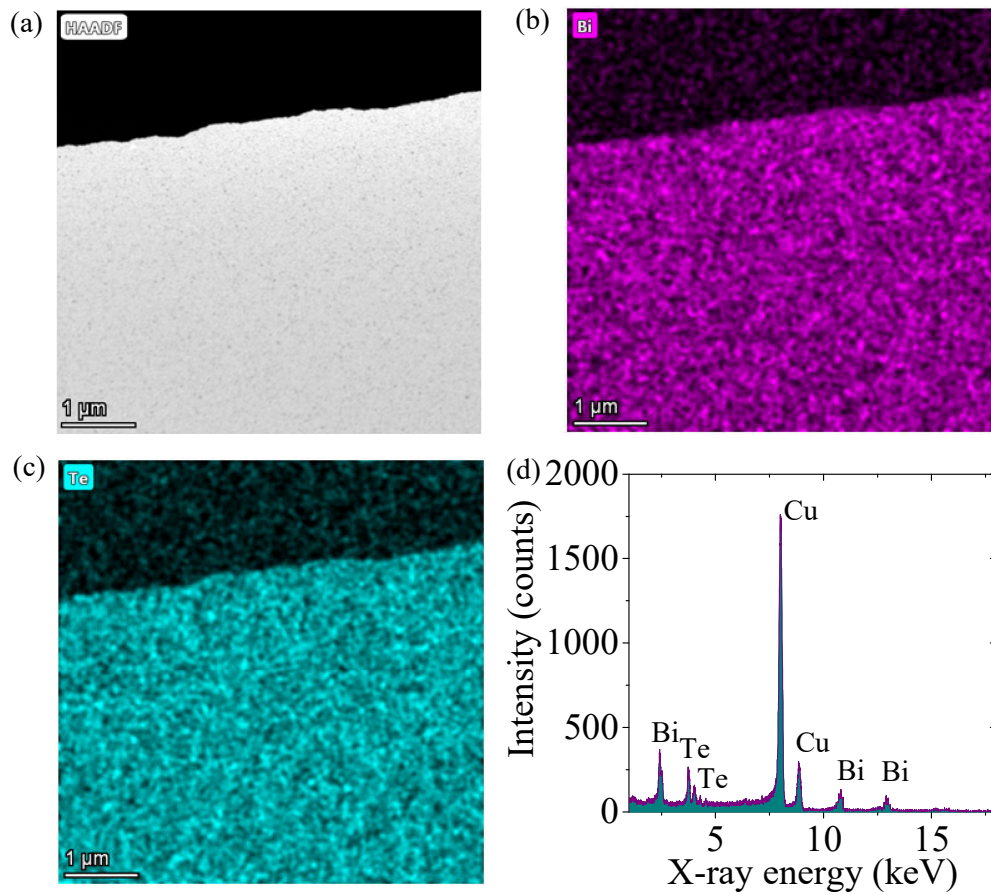
Fig. S4 (a) TEM high-angle annular darkfield (HAADF) image of a 42 nm Bi_2Te_3 TI film transferred on a copper microgrid. (b)-(c) EDX mapping image of a part of Bi_2Te_3 nanofilm for the spatial distributions of elements Bi and Te. (d) Corresponding EDX spectrum of Bi_2Te_3 nanofilm. The atomic ratio of Bi and Te was measured as 41.7: 58.3 (~2:3).
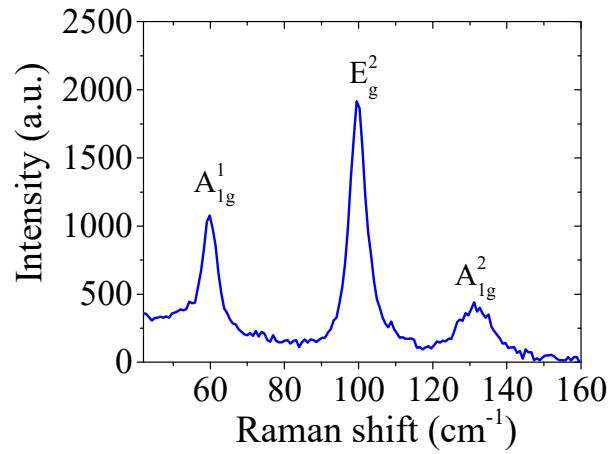
Fig. S5 Raman shift spectrum of Bi_2Te_3 TI measured by using the co-focal micro-spectrometry with a 532 nm laser. The Raman peaks locate at 60, 100, and 131.5 cm^{-1}, which are attributed to the vibrational modes A_{1g}^1, E_g^2, and A_{1g}^2 of Bi_2Te_3 polycrystalline film, respectively.[40]
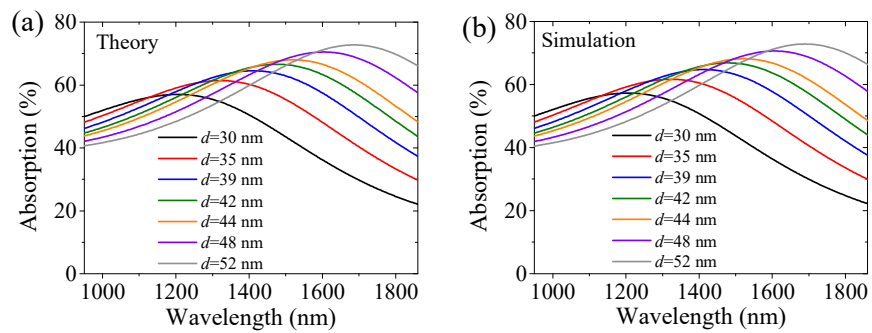

Fig. S6 Theoretically calculated and numerically simulated absorption spectra of TI cavities on a SiO_2 substrate with different Bi_2Te_3 TI film thicknesses d when t=30 nm.
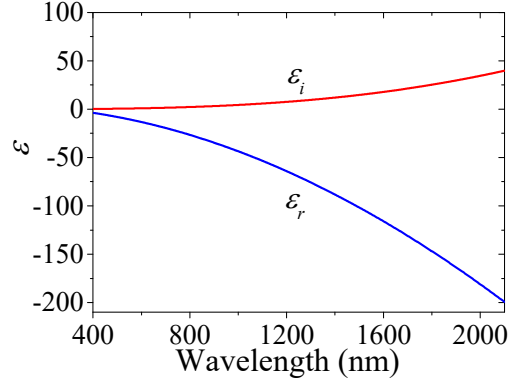
Fig. S7 Relative permittivities of a silver nanofilm deposited by the MS method. The curves were achieved by fitting the ellipsometer data with a Drude model $\varepsilon(\omega)=\varepsilon_\infty-\omega_p^2/[\omega(i\gamma+\omega)]$. The fitted parameters are ε_∞=3.893, ω_p=8.575 eV, and γ=0.116 eV.
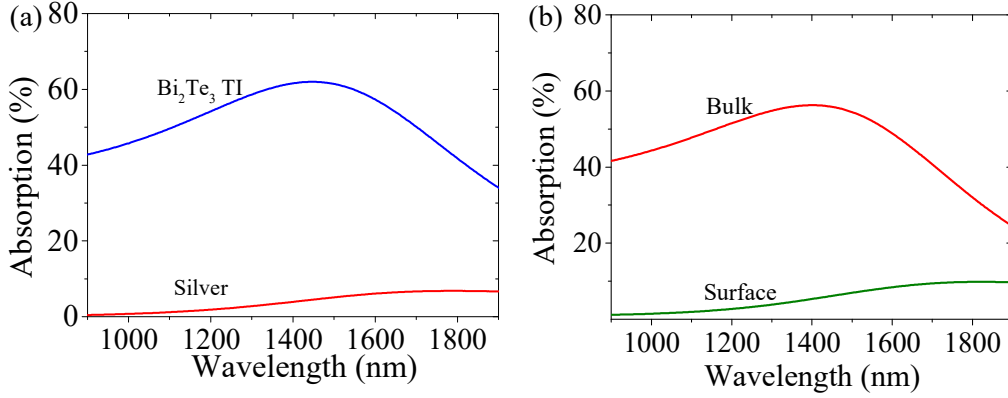

Fig. S8 (a) Absorption spectra of Bi_2Te_3 TI and silver nanofilms in the TI nanocavity with d=42 nm and t=30 nm. (b) Corresponding absorption spectra of the Bi_2Te_3 TI surface and bulk layers.
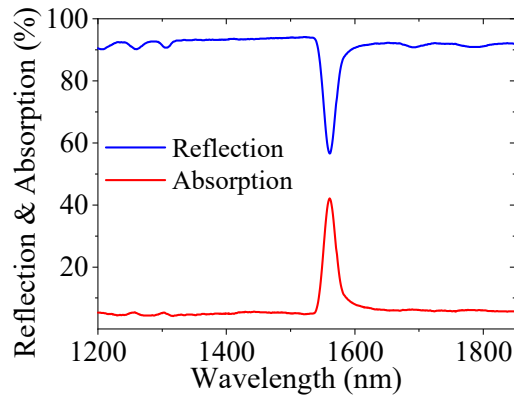
Fig. S9 Experimentally measured reflection and absorption spectra of a 30 nm silver film on the photonic crystal with d_t=182 nm, d_s=260 nm, and N=16.
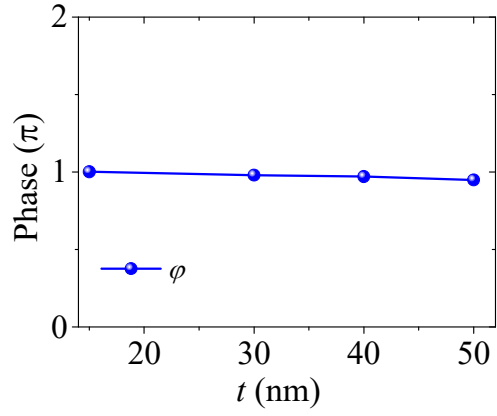
Fig. S10 Coupling phase retardation φ achieved by fitting the measured EIT-like spectra of TI nanocavity/photonic crystal structures with different t.
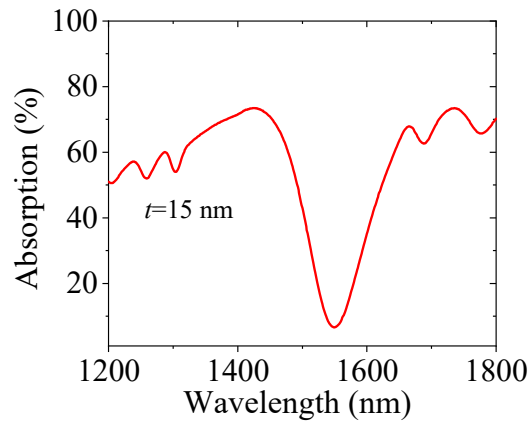
Fig. S11 Absorption spectrum of the Bi_2Te_3 nanocavity/photonic crystal structure with d=44 nm, t=15 nm, d_t=182 nm, d_s=260 nm, and N=16.
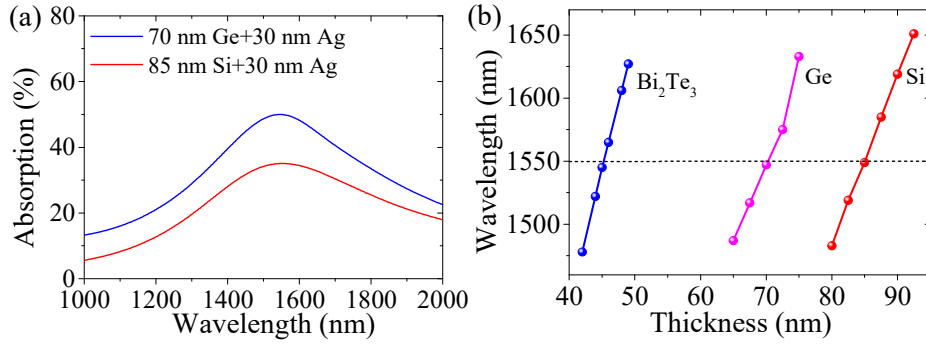
**Fig. S12** (a) Absorption spectra of Si- and Ge-based cavities on the SiO$_2$ substrate. The thicknesses of Ge and Si films on the 30 nm silver layer are 70 and 85 nm, respectively. (b) Dependence of resonant absorption wavelengths on the thicknesses of Si, Ge, and Bi$_2$Te$_3$ films on the 30 nm silver layer. The results were obtained by numerical simulations. In the simulations, we used the experimental data of Si and Ge refractive indices.[59,60]
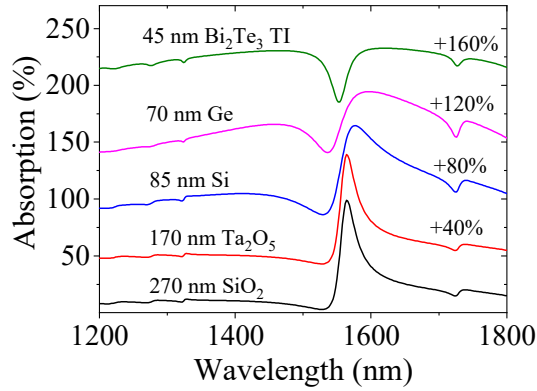
Fig. S13 Absorption spectra of the silver/photonic crystal structures with different material films on the silver layer. Here, t=30 nm, d_t=182 nm, d_s=260 nm, and N=16. The thicknesses of material films are selected with the generation of cavity resonances around 1550 nm.
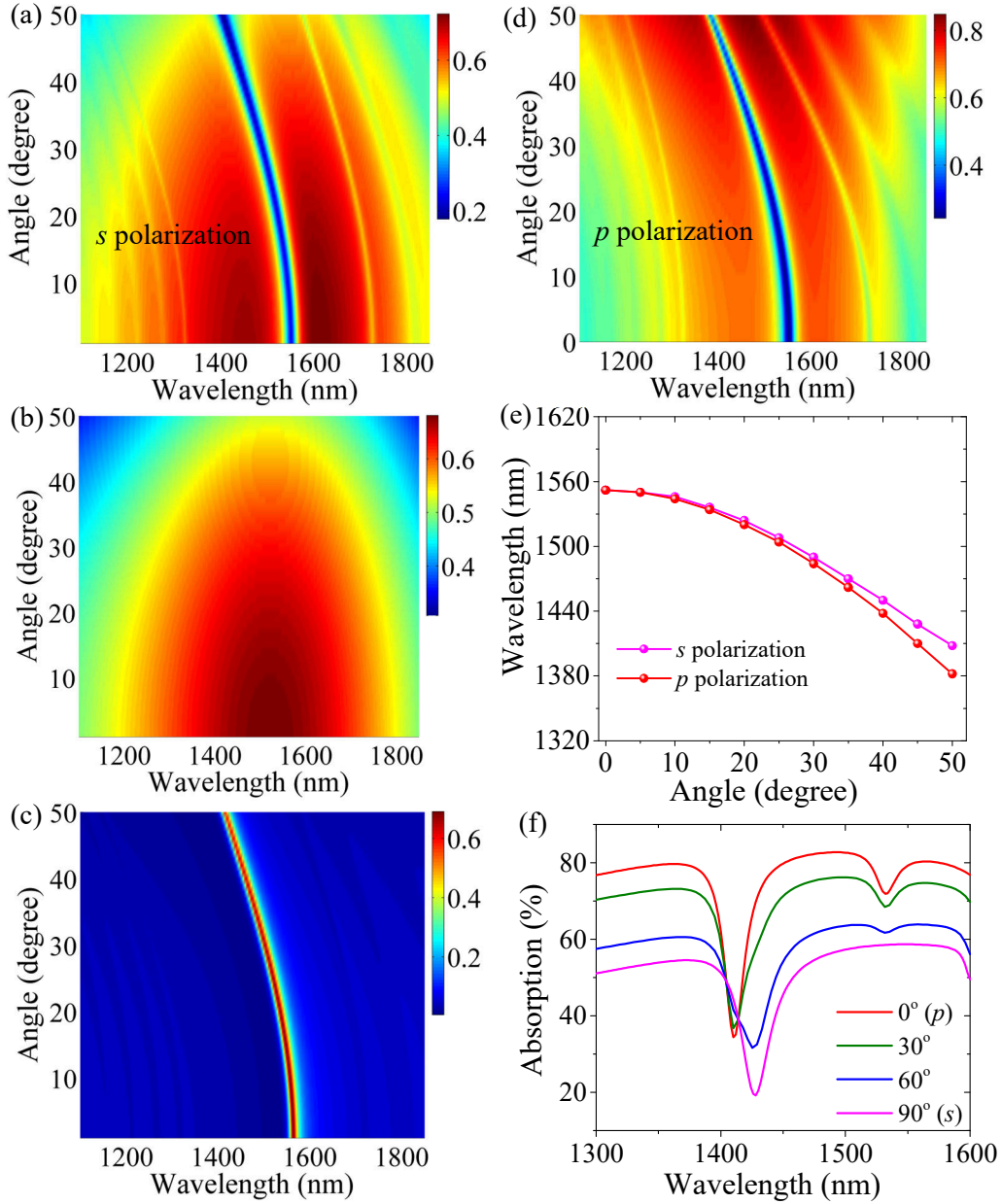
Fig. S14 (a)-(c) Evolution of absorption spectra from TI nanocavity/photonic crystal, TI nanocavity, and silver/photonic crystal structures on the incident angle for *s*-polarized light. (d) Evolution of absorption spectra from TI nanocavity/photonic crystal on the incident angle for *p*-polarized light. (e) Relationship between the induced transparency wavelength and incident angle for *s*- and *p*-polarized light. (f) Absorption spectra from the TI nanocavity/photonic crystal with different polarization angles of light obliquely incident at 45°. Here, the geometric parameters are set as d_t=182 nm, d_s=260 nm, d=44 nm, t=30 nm, and N=16.
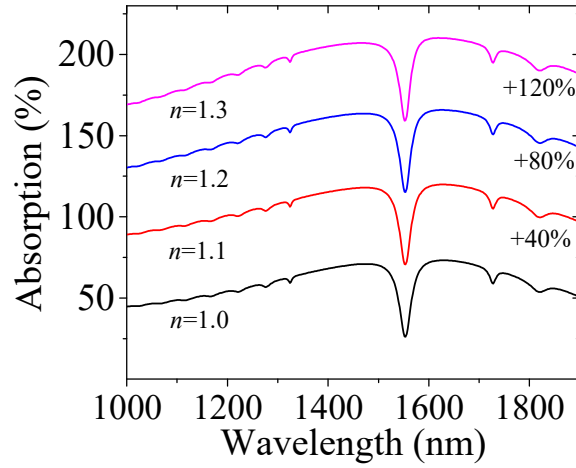
Fig. S15 Absorption spectra of TI nanocavity/ PC structures with the different environmental refractive indices n. Here d=46 nm, t=30 nm, d_r=182 nm, d_s=260 nm, and N=16.
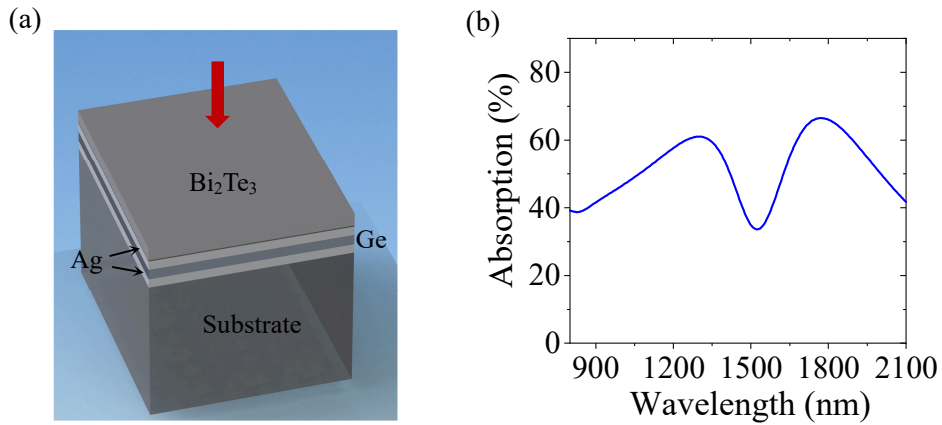
Fig. S16 (a) 3D diagram of Bi_2Te_3 TI nanocavity/Ge/Ag film on a SiO_2 substrate. (b) Absorption spectra of Bi_2Te_3/Ag/Ge/Ag and Ge/Ag/Ge/Ag structures. Here, the thicknesses of Bi_2Te_3 TI, silver, germanium, and silver films are 42, 20, 130, and 20 nm in Bi_2Te_3/Ag/Ge/Ag structure, respectively.

Supplementary Note 1. Preparation of Bi₂Te₃ TI nanofilm for TEM measurement

The preparation of Bi_2Te_3 TI nanofilm for the TEM measurement can described as below. First, a 42 nm Bi_2Te_3 TI film was grown on the SiO_2/Si substrate by using MS deposition. A KOH solution with 1-2 mol/L concentration was dropped on the Bi_2Te_3 nanofilm. After the SiO_2 layer on Si was etched, some fractured Bi_2Te_3 nanofilms will float in the KOH solution. The KOH solution with Bi_2Te_3 nanofilms was dropped into the deionized water. Then, a thin copper microgrid was employed to pick up the small Bi_2Te_3 nanofilms. The copper microgrid with Bi_2Te_3 nanofilms was dried on the heating stage under the temperature of 60 °C. In the TEM, a Bi_2Te_3 nanofilm was chosen to measure the SAED pattern and HRTEM image.

Supplementary Note 2. Spectroscopic ellipsometry measurement of optical constants for Bi₂Te₃ TI material

In the optical range, 3D TI can be normally regarded as a semiconducting (or insulating) bulk covered with a thin metal-like surface layer.[42] The optical constants of TI materials at the frequencies from ultraviolet to near-infrared can be measured using spectroscopic ellipsometer.[42,43] The complex refractive indices (n_b+ik_b and n_s+ik_s) of Bi_2Te_3 TI bulk and surface can be achieved by fitting the spectroscopic ellipsometer data with the Tauc-Lorentz and Drude models, respectively. The bulk relative permittivity ε_b ($\varepsilon_b=(n_b+ik_b)^2$) mainly stems from the interband transition of electrons. For the semiconducting bulk, the band structure can be described using the well-known Kramers-Kronig equations.[44] The bulk relative permittivity ($\varepsilon_b=\varepsilon_b'+i\varepsilon_b''$) can be governed by

$$\varepsilon_b^{"}(E)=\begin{cases} \dfrac{1}{E}\cdot\dfrac{AE_0C\left(E-E_g\right)^2}{E^2C^2+\left(E^2-E_0^2\right)^2}, & E>E_g \\ 0 & E\leq E_g \end{cases} \tag{S1}$$

$$\varepsilon_b'(E) = \varepsilon_{b,\infty} + \frac{2}{\pi} P \int_{E_g}^{\infty} \frac{\varepsilon_b''(\rho)\rho}{\rho^2 - E^2} d\rho, \quad \text{(S2)}$$

where $E=\hbar\omega$ stands for the energy of incident photons, and ω is the angular frequency of photons. A stands for the amplitude of absorption peak. E_0 is the peak in joint density of states, E_g is the band gap energy, and C is the broadening factor. $\varepsilon_{b,\infty}$ represents the high-frequency relative permittivity of bulk. P stands for Cauchy principal part of the integral.[44] The surface relative permittivity ε_s ($\varepsilon_s = (n_s + ik_s)^2$) can be described by employing the Drude model: $\varepsilon_s = \varepsilon_{s,\infty} - \omega_{s,p}^2/(\omega^2 + i\gamma_d\omega)$, where $\varepsilon_{s,\infty}$, γ_d and $\omega_{s,p}$, denote the relative permittivity at high frequency, electron collision frequency, and plasma frequency of surface layer, respectively.[43] By using the ellipsometer, the complex refractive indices of Bi_2Te_3 TI material can be achieved at the angle of 70° for the incident light, as depicted in Fig. 2(d). The layer-on-bulk model can be used to achieve the complex refractive indices of surface and bulk by fitting the experiment data. In Fig. 2(d), it shows that the fitting results agree well with the experimental measurement. The fitted physical parameters in the Drude and Tauc-Lorentz models for the TI surface and bulk states are shown in the Table S1. In this table, we can see that the surface layer thickness was fitted as ~2.29 nm, approaching the estimated thickness of 2.5 nm for 3D TI material.[45] The bandgap energy is ~0.21 eV, close to the reported Bi_2Te_3 bandgap.[46]

Supplementary Table S1. Fitted physical parameters in Drude and Tauc-Lorentz models for the Bi$_2$Te$_3$ TI surface and bulk.

Physical parameters	Fitted values (units)
E_g	0.21 (eV)
$\varepsilon_{b,\infty}$	2.63 (eV)
A	76.64 (eV)
E_0	1.51 (eV)
C	1.71 (eV)
$E_{s,\infty}$	1
$\omega_{s,p}$	7.56 (eV)
γ_d	0.23 (eV)
Surface layer thickness	2.29 (nm)

Supplementary Note 3. TMM theoretical calculations

The transfer matrix method (TMM) can be used to theoretically calculate the propagation of light in multilayer structures.[48] To consider the TI surface and bulk states, the Bi$_2$Te$_3$ nanofilm will be divided into conductor-insulator-conductor trilayer. According to the Maxwell's equations and boundary condition of each layer, the transmission, reflection, and absorption of the multilayer can be achieved. The amplitudes of electric field (E_{j-1}^p and E_j^p) at the upper and lower sides of the j-th interface between the (j-1)-th and j-th layers can be described as

$$\begin{bmatrix} E_{j-1}^{-} \\ E_{j-1}^{+} \end{bmatrix} = \frac{1}{t_j}\begin{pmatrix} 1 & r_j \\ r_j & 1 \end{pmatrix}\begin{bmatrix} E_j^{'-} \\ E_j^{'+} \end{bmatrix} = Q_i \begin{bmatrix} E_j^{'-} \\ E_j^{'+} \end{bmatrix}, \tag{S3}$$

where the superscripts + and – ($p=\pm$) stand for the positive and negative directions of light propagation along y axis, respectively. r_j and t_j represent the reflection and transmission coefficients of light at the interface, which can be respectively obtained by Fresnel equations:

$r_j=(n_{j-1}\cos\theta_j-n_j\cos\theta_{j-1})/(n_{j-1}\cos\theta_j+n_j\cos\theta_{j-1})$ and $t_j=2n_{j-1}\cos\theta_{j-1}/(n_{j-1}\cos\theta_j+n_j\cos\theta_{j-1})$. θ_j and n_j are

the propagation angle of light and refractive index in the j-th layer, respectively. They satisfy

the Snell's law: $n_j\sin\theta_j=n_{j-1}\sin\theta_{j-1}$ ($\theta_0=\theta$). Here, the light is normally incident onto the Bi_2Te_3 TI

nanofilm from air (*i.e.*, $\theta=0^\circ$ and $n_0=1$). The refractive indices of Bi_2Te_3 TI surface and bulk

layers are set as the data in Figs. 2(e) and 2(f), respectively. The amplitudes of electric field at

the upper and lower sides in the j-th layer with the thickness d_j will satisfy the transfer equation

$$\begin{bmatrix} E_j^{'-} \\ E_j^{'+} \end{bmatrix} = \begin{pmatrix} e^{-i\psi_j} & 0 \\ 0 & e^{i\psi_j} \end{pmatrix} \begin{bmatrix} E_j^{-} \\ E_j^{+} \end{bmatrix} = P_j \begin{bmatrix} E_j^{-} \\ E_j^{+} \end{bmatrix}, \tag{S4}$$

where $\psi_i=2\pi n_j d_j\cos\theta_j/\lambda$ is the propagation phase shift of light in the j-th layer. Thus, the input

and output amplitudes of the entire structure can be described as

$$\begin{bmatrix} E_0^{-} \\ E_0^{+} \end{bmatrix} = \left[\prod_{k=1}^{m-1} Q_k P_k\right] Q_m \begin{bmatrix} E_m^{'-} \\ E_m^{'+} \end{bmatrix} = \begin{pmatrix} W_{11} & W_{12} \\ W_{21} & W_{22} \end{pmatrix} \begin{bmatrix} E_m^{'-} \\ E_m^{'+} \end{bmatrix}, \tag{S5}$$

where m is the total layer number. As the input light is only incident on the Bi_2Te_3 TI nanofilm

(*i.e.*, $E_m^{'+}=0$), the transmission, reflection, and absorption of the entire structure can be expressed

as $T=|E_m^{'-}/E_0^{-}|^2=|1/W_{11}|^2$, $R=|E_0^{+}/E_0^{-}|^2=|W_{21}/W_{11}|^2$, and $A=1$-T-R, respectively. As shown in Figs. 3(b)

and S6, the theoretical results are in excellent agreement with the simulations and experiments.